Gas and particle phase polycyclic aromatic hydrocarbon emission factors from a diesel vehicle engine: Effect of operating modes in a developing country context

G. Geldenhuys [a,b], M. Wattrus [c], P.B.C. Forbes [a,*]

[a] *Department of Chemistry, University of Pretoria, Lynnwood Road, Hatfield, Pretoria, 0001, South Africa*
[b] *Impala Platinum Ltd, Processing Laboratory, 123 Bethlehem Drive, Rustenburg, 0299, South Africa*
[c] *Sasol Fuels Application Centre (SFAC), 81 Bridge Place Capricorn Park, Muizenberg, Western Cape, South Africa*

ABSTRACT

Airborne polycyclic aromatic hydrocarbons (PAHs) arising from diesel exhaust emissions are of concern due to their significant human health and environmental impacts. Engine dynamometer experiments with a light duty diesel engine were conducted to measure PAH emissions representative of developing country conditions, and thereby determine emission factors at two different engine operating modes that are representative of idling and severe real-world conditions, respectively. We employed a portable denuder device for the simultaneous sampling of gaseous and particulate PAH emissions, the components of which were subsequently individually thermally desorbed and analysed by two-dimensional gas chromatography with time-of-flight mass spectrometric detection (TD-GCxGC-ToF-MS). Results indicated that PAH emission factors differed significantly for the different modes of engine operation with the highest emission factor being for idle mode with a total PAH emission factor of 1181.14 µg/kg. Under real-world conditions, it is expected that further variance in emission factors will be introduced as a result of brake and tyre wear, different engine technologies, engine age and maintenance, as well as fuel quality and measurement methods.

1. Introduction

Air pollution emissions from mobile sources need to be monitored to evaluate the efficiency of regulatory measures, maintain accurate emission inventories and also to assess the potential impact that transportation has on human and environmental health. Diesel exhaust emissions (DEE), in particular, have been classified as being carcinogenic based on comprehensive laboratory experimental findings and epidemiological studies that have reported strong associations between vehicle emissions and adverse health impacts (Kim et al., 2013; Rengarajan et al., 2015; Samet et al., 2000; Shen et al., 2014, US EPA, 2004, 2014). Notably, the International Agency for Research on Cancer (IARC) has established that diesel emissions may induce lung cancer and be associated with an increased risk of bladder cancer (IARC 2012).

DEE comprises of a complex mixture of compounds and its composition is dependent on various parameters such as engine technology, fuel type, temperature, humidity, mode of engine operation and maintenance (Weitekamp et al., 2020). The gaseous fraction of DEE consists of carbon monoxide, carbon dioxide, nitrogen oxides, sulphur oxides, and volatile organic compounds. The particulate fraction includes elemental and organic carbon (EC and OC), sulphates, and metals. As a result, diesel combustion emissions contribute to ambient particulate and gaseous air pollutant levels, including those of polycyclic aromatic hydrocarbons (PAHs) (Ono-Ogasawara and Smith, 2004).

PAHs are semi-volatile organic compounds that can be distributed over both fractions of the exhaust, depending on operating and environmental conditions (Vione et al., 2004). Some PAHs have been found to be toxic and even carcinogenic to humans, and therefore their regulation and quantification in each phase is crucial (Rohr and Wyzga, 2012 (Reşitoğlu et al. 2015)). The United States Environmental Protection Agency (US EPA) has identified 16 priority PAHs as illustrated in Table 1 and the World Health Organization (WHO) added 17 additional PAHs to make a total of 33 PAHs under its regulation (Poster et al., 2006, WHO, 2014). The different sources of PAHs in diesel vehicle exhaust include unburned fuel, lubricating oil and pyrosynthesis from lower molecular weight aromatics originating from the fuel (Rhead and Pemberton,

Table 1

Sixteen US EPA priority PAHs and their corresponding abbreviations, molar masses and boiling points (PubChem database, Available at https://pubchem.ncbi.nlm.nih.gov/compound).

	Formula	PAH Name	Abbreviation	Molar Mass (g/mol)	Boiling point (°C)
1	$C_{10}H_8$	Naphthalene	Nap	128	218
2	$C_{12}H_8$	Acenaphthylene	Acy	152	265
3	$C_{12}H_{10}$	Acenaphthene	Ace	154	278
4	$C_{13}H_{10}$	Fluorene	Flu	166	295
5	$C_{14}H_{10}$	Phenanthrene	Phe	178	339
6	$C_{14}H_{10}$	Anthracene	Ant	178	340
7	$C_{16}H_{10}$	Fluoranthene	FluAn	202	375
8	$C_{16}H_{10}$	Pyrene	Pyr	202	360
9	$C_{18}H_{12}$	Benz[a]anthracene	BaA	228	435
10	$C_{18}H_{12}$	Chrysene	Chy	228	448
11	$C_{20}H_{12}$	Benzo[b]fluoranthene	BbF	252	481
12	$C_{20}H_{12}$	Benzo[k]fluoranthene	BkF	252	481
13	$C_{20}H_{12}$	Benzo[a]pyrene	BaP	252	495
14	$C_{22}H_{12}$	Benzo[ghi]perylene	BghiP	276	536
15	$C_{22}H_{12}$	Indeno[1,2,3-cd]pyrene	I123P	276	536
16	$C_{22}H_{14}$	Dibenz[ah]anthracene	DbahA	278	524

1996). PAHs in unburned diesel fuel have been shown to be the primary contributor of lighter 2–3 ringed PAHs in diesel exhaust. For example, 24% of naphthalene in the exhaust was found to be sourced from naphthalene in the fuel that survived combustion (Marr et al., 1999). It was also concluded that the presence of higher molecular weight PAHs in diesel exhaust, not present in the fuel, originate from other sources such as lubricating oil or pyrosynthesis (Marr et al., 1999).

Vehicle emission factors (EFs) are functional relationships that predict the quantity of an emitted pollutant as a function of the activity causing the emission (Phuleria et al., 2006; Riccio et al., 2016). EFs are significantly influenced by factors such as vehicle type; engine age and maintenance; fuel type and composition, as well as driver behaviour and travel speed. Poor fuel quality, aging vehicle fleet, and lack of roadworthy emission tests and operational maintenance are the reasons for the lack of standard compliance and for higher that normal transport emissions in developing countries (Ayetor et al., 2021). It is for this reason that there continues to be a need to characterize the potential health risks from older engines which are prevalent in developing countries, and it is also vital assess health and environmental effects associated with exposure to diesel exhaust as a whole (Weitekamp et al., 2020).

EFs have been measured using a number of different methods, including vehicle chassis dynamometer studies (Yanowitz et al., 1999; Kostenidou et al., 2021), remote sensing (Burgard et al., 2003; Guo et al., 2007; Schifter et al., 2003; Zhang et al., 1995), twin-site experiments (Gietl et al., 2010; Oliveira et al., 2010; Pey et al., 2010), roadway tunnel studies (Phuleria et al., 2006; Kristensson et al., 2004; Handler et al., 2008; Mancilla and Mendoza, 2012; Weingartner et al., 1997; Abu-Allaban et al., 2002; Wang et al., 2021) and on-road chase experiments (Wang et al., 2011) each of which have their advantages and limitations which are comprehensively reviewed by Vicente Franco et al. (2013).

Riccio et al. determined PAH emission factors from an urban tunnel experiment in Naples, Italy whereby they placed two mobile measuring stations at the entrance and exit of the tunnel and took PM_{10} samples every hour onto 47 mm borosilicate glass filters (Riccio et al., 2016). The authors found PAH concentrations as high as 1450 ng/m^3, with benzo(a)pyrene having an EF of 2.7 μg/km, which was three times higher than expected based on other studies. Lower molecular weight PAHs, i.e., 3-ring PAHs, were abundant at both the tunnel entrance and exit, while

the most prevalent PAHs were the 4-ring pyrene and benzo(a)anthracene and the 6-ring dibenzopyrenes (Riccio et al., 2016).

Tunnel measurements of PAHs lack resolution on individual vehicle contributions as they represent the overall vehicle fleet emissions in a specific tunnel and sources are not limited to exhaust emissions alone but also include emissions from other sources such as grassland fires, domestic fires and industry emissions. Additionally, transient ambient tunnel sampling methods only cover limited traffic circumstances and are influenced by changes in the local meteorological and environmental conditions and the results may not be generally applicable to open roadways (Ning et al., 2008). Another consideration to be made in tunnel EF studies is that the sampled air mass may be fresh or aged, or a mixture of the two, which will impact the speciation of pollutants (Forbes et al., 2013).

Zheng et al. (2017) employed a portable emissions measurement system (PEMS) to collect real-world particle samples from diesel vehicles in China. DPM samples were collected onto 47 mm quartz fiber filters with a cyclone filter impactor with inlet flow rate of 5 L/min. Fourteen in-use heavy-duty diesel vehicles were employed in the study to measure the species-resolved particulate PAH emissions under real-world driving conditions and 15 priority PAHs were characterized by gas chromatography-mass spectrometry (GC-MS). The authors found that 3 and 4-ring PAHs accounted for 95% of the total measured particulate PAH emission factors for all vehicles. They also noted that the average particulate emission factor of 15 PAHs for electronically controlled fuel injection engines was 187 ± 80 μg/kg which was a 76% reduction when compared to 782 ± 378 μg/kg for mechanical pump fuel injection engines, which clearly indicated the influence that engine technology has on emission factors (Zheng et al., 2017).

For a study to determine EFs to be effective and accurate, it should be performed under realistic driving conditions where the inputs from other sources are minimized. Modern dynamometers can realistically vary load on the vehicle or engine to simulate real world driving and can produce realistic brake wear when driven through a transient driving cycle, however a limitation of this type of study is that a controlled laboratory environment will never fully represent real-world driving conditions (Cocker et al., 2004, Zheng et al., 2016). Another consideration is that dynamometer studies cannot fully replicate other inevitable non-exhaust emissions such as those from the wear of brake linings, tyre wear and re-suspended road dust, all of which will contribute to roadside emissions (Abu-Allaban et al., 2003, Allen et al., 2001, Morawska and Zhang, 2002).

In a recent study, PM emitted from diesel vehicles operated under different driving conditions on a chassis dynamometer revealed that the emissions were dominated by the organic carbon fraction whereby the PAH analysis results revealed that 4 and 5-ring PAHs were the most prevalent (Wang et al., 2021). The sum of particulate PAH EFs ranged widely from 0.41 to 18.60 mg/kg for the different vehicles tested in the study, of which most of were Euro 4 and 5 compliant (Wang et al., 2021).

In a comprehensive review of literature, whereby exposure to both filtered and whole diesel exhaust was considered, it was found that the gas fraction of diesel exhaust plays a significant role when considering health-related endpoints (Weitekamp et al., 2020). The numerous studies cited in this article, and others found in the literature, have primarily paid attention to the toxicity of particulate matter and soot emissions, but it has been found that many PAHs are emitted predominantly in the gas phase (Geldenhuys, 2014; Geldenhuys et al., 2015). The methods cited in literature use sampling methods that require larger sampling volumes and extended sampling times to accurately quantify trace level of PAHs in ambient air, after which a highly sensitive analytical system must be employed after complicated and time consuming pre-treatment and analyte concentration procedures (Pandey et al., 2011). All of the aforementioned sampling strategies introduce unwanted sampling artefacts and increase the risk of analyte breakthrough and blow off resulting in vital PAH partitioning

information being lost. It is for this reason that it is vital to overcome these sampling bottlenecks and include a simplified sampling method that is able to adopt low flow rates, short sampling intervals and simultaneous sampling of gas and particle phase PAHs in a manner in which their partitioning is unaffected by sampling conditions. Correspondingly, the aim of this study is to determine gas and particulate phase PAH emission factors from a light duty diesel engine, in a controlled test cell facility, which is operated at two different modes representative of different engine operating conditions. It is the first time that both gas and particle PAH EFs have been simultaneously determined for different engine operating modes using small portable denuder sampling devices that minimise sampling artefacts and avoid time consuming and environmentally unfriendly sample preparation techniques. These phase specific EF values will be useful in the calculation of more accurate emission inventories and can be used to guide air quality management plans as well as reduction and abatement strategies. Gas and particle phase PAH profiles and EFs at each of the modes tested are then compared to other reported studies using other measurement methods (such as tunnel and roadside samples) in order to assess the advantages and disadvantages of the adopted test measurement strategy and identify potential areas of further development.

2. Methodology

Controlled testing was carried out at the Sasol Fuels Application Centre in Cape Town, South Africa. Vehicle emissions were simulated and tested in a test cell equipped with a Euro 2 compliant, 1.6 L test engine, fitted with a close-coupled diesel oxidation catalyst (DOC). Diagnostic checks were carried out on the engine prior to testing to ensure performance was as per specification. It must be noted that poor fuel quality, an aging vehicle fleet, and lack of mandatory roadworthy emission tests are reasons which can contribute to the lack of standard compliance in developing countries in Africa (Ayetor et al., 2021). It is for this reason that a Euro 2 compliant engine was chosen to be representative of the average fleet in developing countries, and the emissions arising from this engine would have significance in, for example, South Africa where the Euro 2 Vehicle Emission Standard is adopted.

The test fuel contained less than 10 ppm sulphur and the test engine operation modes, dynamometer details and fuel specifications are listed in Tables 2–4 respectively. An electrical engine dynamometer was coupled to the test engine to simulate and control engine operation parameters, including speed, torque and throttle and all the testbed data as well as engine control module (ECM) parameters were logged by the test cell automation system at a frequency of 10 Hz. Fig. 1 shows a schematic of the test cell setup. Fuel consumption was measured using a mass flow meter employing a Coriolis mass flow sensor and fuel temperature conditioning unit (AVL models 735S and 753C, respectively).

The test engine was operated in 2 different operating modes as detailed in Table 2. These modes represent varying torque (power) conditions. M_A represents a vehicle idling whilst M_B represents a vehicle exerted to maximum power and speed i.e., driving uphill whilst pulling a load. The actual operating modes of vehicles on the road would fall within the range of these test modes, seeing that M_B is a severe operating mode, allowing for a predicted range of emissions to be estimated.

2.1. Test engine

The test engine was a 1.6 L engine which is used in light duty

Table 3
Test engine specifications.

Parameter	Detail
Model year	2010
Cylinders	4
Capacity	1,595 cm^3
Compression ratio	16.5 : 1
Induction	Turbocharged with intercooler
Fuel System	Common rail direct injection using piezo injectors
Exhaust gas recirculation	Cooled exhaust gas recirculation (EGR) for NO$_x$ control
Transmission	5-speed manual
Max Power	77 kW @ 4400 rpm
Max Torque	250 Nm @ 1500–2500 rpm
Emission control	Close-coupled diesel oxidation catalyst (DOC)
Emission level	Euro 2
CO$_2$ emissions	109 g/km

Table 4
Test fuel specifications.

Carcal RF-06-03	
Cetane number	53.5
Density at 15 °C (g/mL)	0.8363
Aromatics (% volume)	26.9
Flash point (°C)	83
Polycyclic aromatic hydrocarbons (% mass)	5.0
Viscosity at 40 °C (mm^2/s)	2.75
Sulphur (mg/kg)	1.2
Lubricity at 60 °C (μm)	376
Water content (mg/kg)	70
Carbon content (% mass)	86.70
Hydrogen content (% mass)	13.30

passenger vehicles and it is Euro 2 emission level compliant. The engine was set up using a production standard engine Electronic Control Unit and exhaust system. The engine was fitted with a Diesel Oxidation Catalyst (DOC) which is typical for a Euro 2 emission level engine as used in vehicle fleets found in developing countries. Further details of the test engine are shown in Table 3.

2.2. Test fuel

For the test cell experiments, an ultra-low sulphur (ULS) diesel fuel that contained less than 10 ppm sulphur was used during testing (Carcal RF 06–03). This certification test fuel was sourced from Europe, and is EN590 compliant. The specifications of the test fuel are presented in Table 4.

2.3. Laboratory analytical equipment

Undiluted exhaust gas was sampled using a Horiba MEXA series 7000 exhaust gas analyser to measure concentrations of NOx (nitrogen oxides), CO (carbon monoxide), THC (total hydrocarbons), and CO$_2$ (carbon dioxide). Real-time measurements of soot concentration in the undiluted exhaust were performed by means of a photo-acoustic soot sensor (AVL483 Micro Soot Sensor). Soot measured in this way corresponds to the insoluble or non-volatile portion of the particulate matter (primarily elemental carbon). DPM emissions are typically expressed in grams of particulate matter per unit of mechanical energy delivered by the engine, such as g/kWh. This approach normalises DPM with
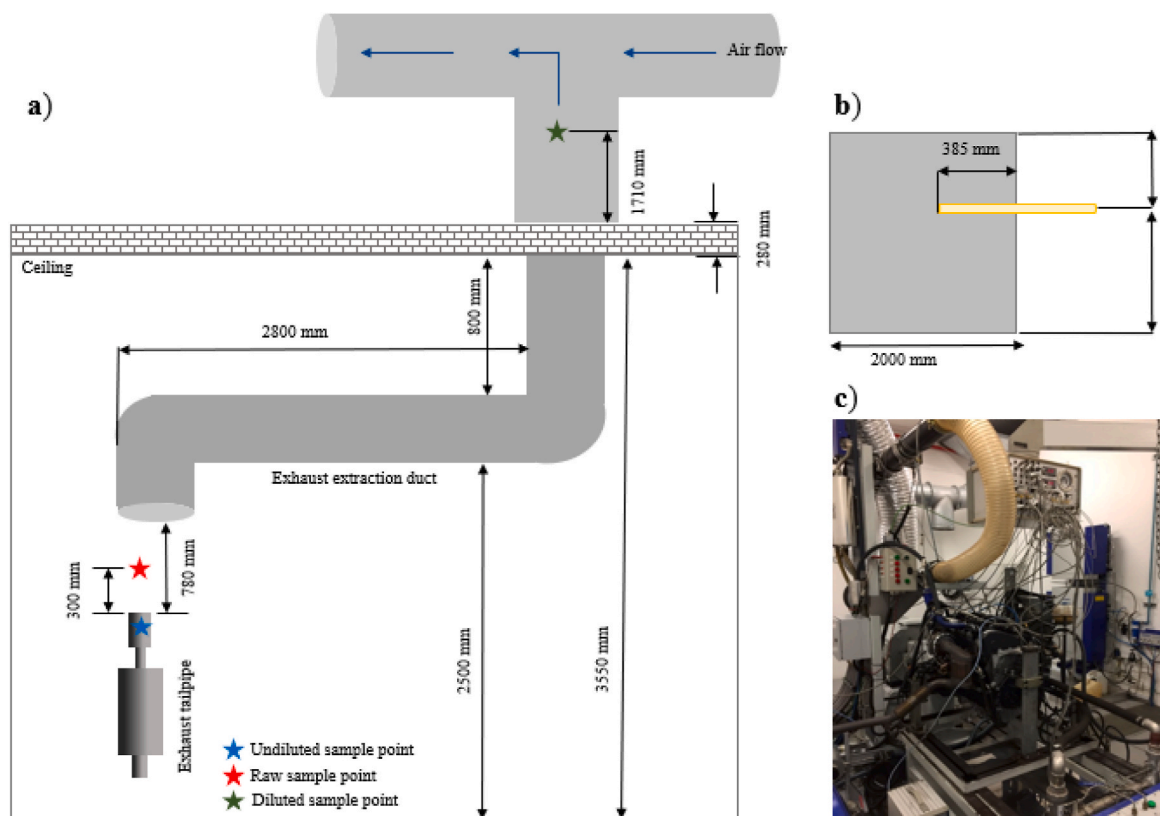
Table 2
Test engine operation modes.

	Dyno Speed (rev/min)	Brake Power (kW)	Dyno Torque (Nm)	Engine Throttle Position (%)	Fuel Mass Flow Rate (kg/h)	Intake Air Mass Flow (kg/h)	Exhaust Mass Flow Rate (kg/h)
M_A	780	4.19	10	27.4	3.13	232	235
M_B	4000	78	187	100	18.4	399	417

Fig. 1. (a) Schematic of test cell setup indicating the undiluted, raw and diluted sample positions, (b) cross section of diluted sample position in the exhaust duct and (c) a photograph of the test cell setup.

mechanical energy and thus removes any variability between tests introduced by variable exhaust flow rates or engine power differences. No correction for thermophoretic or diffusional losses has been applied to the measured results. These instruments for the measurement of exhaust emissions are done according to international standard methods. The humidity and ambient pressure in the test cell were determined with a Kestrel portable weather station.

On-line instruments sample undiluted exhaust gas from the inside of the tailpipe. In addition, a sampling point was positioned at a distance of 0.3 m away from the tailpipe exit. This optimum distance of 0.3 m was determined by measuring the soot and gas emissions at different distances from the tailpipe outlet in order to balance variability in dilution ratio while satisfying the concentration and temperature range of the sampling devices. The samplers that were positioned 0.3 m away from the tailpipe outlet, were named "Raw" as opposed to the measurements that were taken directly in the tailpipe to measure undiluted exhaust emissions which were named "Undiluted".

A select number of measurements were taken in the exhaust extraction duct of the facility. The raw exhaust passed into the exhaust extraction duct before it was emitted to the outside atmosphere. The diluted measurements were taken directly in the exhaust duct with minimal adjustments and they represent a more aged and equilibrated air mass (Fig. 1). Samples were taken after ~4 min equilibration in each mode. A background air sample was also taken from the inlet air that was supplied to the test cell after it had passed through fabric filters. The position of the sample was approximately 0.3 m inside the inlet ducting.

2.4. Sampling methodology

PAH sampling was performed at two positions during each mode: 1) On a stand parallel to exhaust flow at a distance of 0.3 m from the tailpipe exit, denoted "Raw", and 2) On a probe in the exhaust extraction duct perpendicular to air flow denoted "Diluted".

Particle and gas phase PAH sampling was performed using multi-channel silicone rubber trap denuders (Fig. 2). The PAH samples were collected at a flow rate of 500 mL/min for 10 min, using Gilair Plus personal sampling pumps (Sensidyne), to obtain a final sampling volume of 5 L.

The denuder consisted of two multi-channel silicone rubber traps (each trap: 178 mm long glass tube, 6 mm o.d., 4 mm i.d.) each containing 22 parallel PDMS tubes (55 mm long, 0.3 mm i.d., 0.6 mm o.d.) separated by a 6 mm diameter quartz fibre filter (QFF), held in position by a Teflon connector. This configuration allows for both gas and particulate phase sampling (Forbes et al., 2012; Forbes and Rohwer, 2009, 2015; Munyeza et al., 2019). In the denuder, the gas phase SVOCs are trapped by the first (primary) trap as the polydimethysiloxane serves as a solvent for these compounds, and the particles are trapped downstream on the quartz fiber filter. The post filter trap (secondary trap) collects any PAHs that break through from the primary trap or have blown off from the filter. Fig. 2 illustrates the sampler setup.

2.5. Instrumental analysis

Offline analysis of the denuders was performed by means of a LECO Pegasus 4D GCxGC-ToFMS instrument (LECO, St. Joseph, MI, USA) that was equipped with an Agilent Technologies 7890 GC (Palo Alto, CA, USA), a quad jet dual-stage modulator and a secondary oven. Data acquisition and processing was executed by ChromaTOF software version 4.0 (LECO Corp., St. Joseph, MI). A Gerstel 3 Thermal Desorption System (TDS) was employed for sample introduction. Synthetic air was used for the hot jets and liquid nitrogen (LN$_2$) was used to cool nitrogen gas for the cold jets with an AMI Model 186 liquid level controller to maintain sufficient levels. The GC column set consisted of a Restek Rxi-1MS nonpolar phase 100% dimethyl polysiloxane; (30 m, 0.25 mm i.d., 0.25 μm df) as the first dimension (1D) and a Rxi-17Sil MS, midpolar 5% phenyl 95% methylsiloxane (0.79 m, 0.25 mm i.d., 0.25
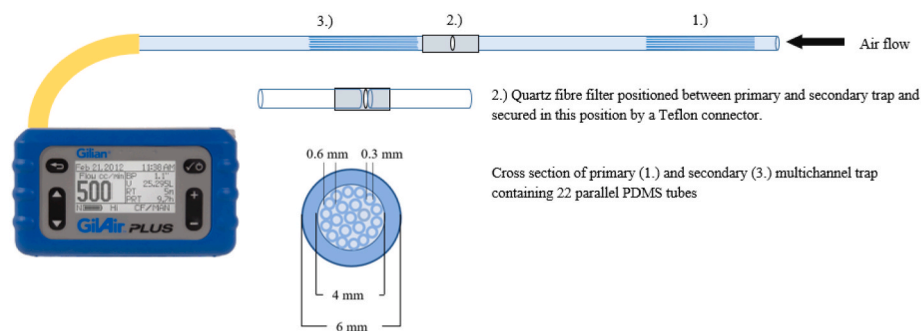
Fig. 2. Schematic of multi-channel trap denuder sampling devices used for PAH sampling.

μm df) as the second dimension (2D). Thermal desorption was carried out from 30 °C to 280 °C at 60 °C/min and held for 5 min after which the analytes were cryogenically focused via a cooled injection system (CIS) at −50 °C using liquid nitrogen. The temperature was ramped at 12 °C/s to 280 °C and the inlet purge time was 3 min. The desorption flow rate was 100 mL/min and the TDS transfer line was at 280 °C. The primary oven was ramped at 10 °C/min from 40 °C to 315 °C which was held for 5 min. The secondary oven was offset by +5 °C and the modulator temperature was offset by 30 °C. The modulation period was 4 s with a hot pulse time of 1 s. The MS transfer line temperature was set to 280 °C and mass acquisition ranged from 50 to 500 Da at 100 spectra/s. The electron energy was 70 eV and the ion source temperature was 200 °C.

2.6. Matrix matched calibration standards

Calibration was performed by using a certified standard PAH mix solution (Supelco, St Louis, MO), containing 15 priority PAHs (Table 1 with the exception of benzo[k]fluoranthene). The nominal concentration of each compound in the mixture dissolved in methylene chloride was 2000 μg/mL. The names and abbreviations of the PAHs included are given in Table 1. Stock solutions at a concentration of 100 μg/mL were prepared in toluene and working solutions were prepared by appropriate dilutions of the stock solutions before use. All solvents used for standard preparation and cleaning of syringes, traps and filters, were of analytical grade (99% purity) including toluene, DCM and n-hexane which were purchased from Sigma Aldrich. Acetone was obtained from Associated Chemical Enterprises, (ACE South Africa). Deuterated internal standards (I_{Std}), d8-naphthalene, d10-phenanthrene, d10-pyrene and d12-chrysene were obtained from Isotec Inc (Sigma Aldrich, Bellefonte, USA) and used in all standards and samples.

Calibration curves were generated in order to quantify gas and particle phase PAHs. For gas phase PAHs, quantification was achieved by analysing individual conditioned PDMS traps that were spiked with 1 μL of the following concentrations of mixed PAH standard in toluene: 1.0, 2.0, 5.0, 10.0 and 15.0 ng/μL. Similarly, to quantify particle bound PAHs, clean 35 mm QFF punches were spiked with 1 μL of 0.5, 1.0, 2.0, 3.0, 5.0 and 10 ng/μL mixed PAH standards in toluene. The I_{Std} mixture, containing d8-naphthalene, d10-phenanthrene, d10-pyrene and d12-chrysene (1 ng/μL), was spiked onto all samples prior to analysis and calibration curves were derived using the area ratio of target analyte: I_{Std}. The I_{Std} correction accounted for any instrument variability or matrix effects. Linear regression analyses were performed after blank correction, using the Data Analysis Toolkit in Excel. The limit of detection (LOD) of each target compound was calculated as a response at three times the signal to noise (S/N) ratio and the limit of quantitation (LOQ) as ten times the S/N ratio.

2.7. Test cell measurements

Temperature and air flow within the test cell were monitored via online sensors. Air flow was measured using a thermal mass flow sensor

(ABB Sensyflow) connected to the engine air intake and the exhaust flow rate was calculated on the basis of the conservation of mass, by adding the intake air and fuel mass flow rates together. The temperature sensors included a wall mounted sensor for an overall test cell temperature, a sensor at the intake filter of the engine and a sensor in the exhaust stream at the sample point 0.3 m away from the tailpipe (raw sample point). Fig. 3 depicts the temperature as a function of varying engine power. The humidity in the test cell was 46% and the ambient pressure was 1021 Pa.

The distance of 0.3 m from the tailpipe was selected as it was close enough to the source for stable engine readings based on monitored CO_2 and NO_X emission dilution factors (less variability as depicted in Fig. 4) and was far enough from the tailpipe for sampling devices to withstand elevated temperatures from the exhaust. The temperature at the sampling point (inlet of denuder) ranged from 46 °C at 50% load to 53 C after running for a short while at maximum load, which later increased to 210 °C. Fig. 4 depicts the decreasing engine variability at distances from −0.1 m (penetrating the tailpipe) to 0.5 m from the tailpipe for CO_2 and NO_x emissions.

Fig. 5 shows the emission of common pollutants as a function of engine power. It is clearly visible for each pollutant, that the engine operation mode significantly influences the concentration of pollutants emitted which are largely governed by the high temperatures and pressures of the combustion process as well as the air-to-fuel ratio, which varies due to the lean-burning nature of diesel engines. Total hydrocarbons are found in highest concentration in idle mode which is characterized by oxygen rich conditions and the lowest at the maximum power mode. The opposite trend was seen for soot emissions where concentrations were elevated to approximately 44 mg/m^3 during maximum power mode which can be attributed to the increase in temperature and oxygen deficient conditions. The NO_x emissions reveal a similar progressive increase in emissions as the engine torque is increased as this causes an increase in temperature which increases NO formation kinetics (Eiguren-Fernandez and Miguel, 2012). CO_2 emissions increase purely as a function of the amount of fuel burned and
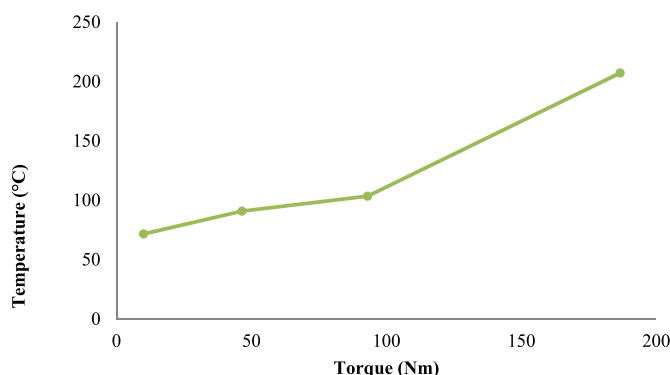

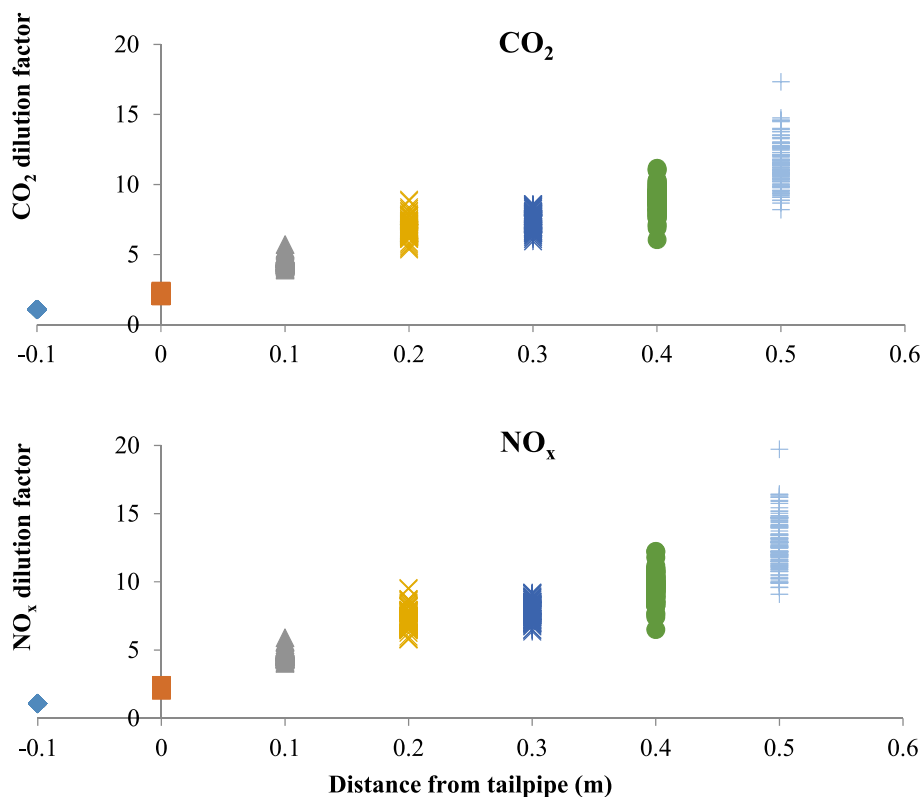**Fig. 3.** Torque measurements as a function of temperature.

Fig. 4. Variation in engine emission dilution factors as a function of sampling distance from the tailpipe outlet.

since the engine load is progressively increased, the amount of fuel burned and therefore CO_2 emitted also increases. In Section 3.2 these results are correlated to PAH emissions to gain a better understanding of the concentrations emitted and the phase partitioning thereof.

3. Results and discussion

3.1. Calibration results

Table 5 represents the 10 out of 15 priority PAHs that were detected in the gas and particle phase samples with their abbreviations. The R^2 values show good linearity but were affected by variation in TD efficiency.

Table 6 shows the limits of detection and quantitation for PAHs on the multi-channel PDMS traps (gas phase PAHs) and on quartz fibre filter (particulate phase PAHs). The LOD and LOQ are given in pg on trap as well as ng/m^3 based on a sample volume of 5 L. The limit of detection (LOD) of each target compound was calculated as three times the signal to noise (S/N) ratio and the limit of quantitation (LOQ) as ten times the S/N ratio. These values were found to have similar orders of magnitude to the values reported in another study that saw the application of the denuder devices in an underground platinum mine (Geldenhuys et al., 2015). The limit of detection for the gas phase PAHs range from 0.3 ng/m^3 for 2 ringed naphthalene to 79.3 ng/m^3 for 6-ring benzo(ghi) perylene. The LOD for the particulate bound PAHs ranged from 0.3 ng/m^3 for naphthalene to 18.5 ng/m^3 for dibenz(a,h)anthracene.

3.2. Total gas and particulate PAH concentrations

Total PAH emissions from the raw exhaust were 6.3 and 33.9 $\mu g/m^3$ for M_A (idle mode) Raw and M_B (max power mode) Raw, respectively and 0.2 and 21.7 $\mu g/m^3$ for the dilute samples as seen in Table 7. From Fig. 6 it can be seen that PAHs were predominantly found in the gas phase (80–100% in the raw exhaust stream as well as in the dilute (aged)

samples). There were no ambient PAHs detected in the background samples.

The raw M_A sample showed that over 90% of PAHs were detected on the primary trap and only 10% on the secondary trap, with no particulate PAHs, whilst the diluted sample revealed that 0.25 $\mu g/m^3$ of PAHs were detected solely on the primary trap. The raw M_B sample showed gas and particulate PAHs which is consistent with denuder theory in which the primary PDMS trap acted as a solvent for the gas phase analytes and analytes that were associated with particles passed through the trap and were collected on the downstream filter and either remained on the filter or subsequently experienced blow off and were then trapped on the secondary trap). Blow off (or loss by volatilization) is a well-documented phenomenon, whereby loss of particle phase analyte is caused by the pressure (and temperature) gradient existing through the filter (Kumari and Lakhani 2018). The loss due to blow off is expected to be minimal due to low sampling flow rates and sampling times, however it can still occur and should be taken into account via the use of a second trap in this case. In addition, the low back pressure across the denuder sampling device throughout this sampling interval reduced the potential for such effects to occur.

M_B showed much higher PAH concentration than the idle M_A which is expected as the engine was under load (full throttle and full torque). The raw sample showed higher concentrations of PAHs on the secondary trap than the primary trap which is due to blow off from the filter and PAHs that are transiently associated with particles when exiting the exhaust since there is not sufficient time to equilibrate. The gas/particle partitioning of PAHs is complex and is also further influenced by the high temperatures of the exerted engine in M_B, which perturbs the equilibration between phases.

Particulate emissions were the highest for M_B which correlated to the highest soot and carbon dioxide emissions in the test cell measurements (Fig. 5) which suggests that soot measurements may be used as a proxy to estimate particulate PAHs levels in diesel emissions. During sampling for M_B, less than 1 L of raw emissions were sampled due to pump failure
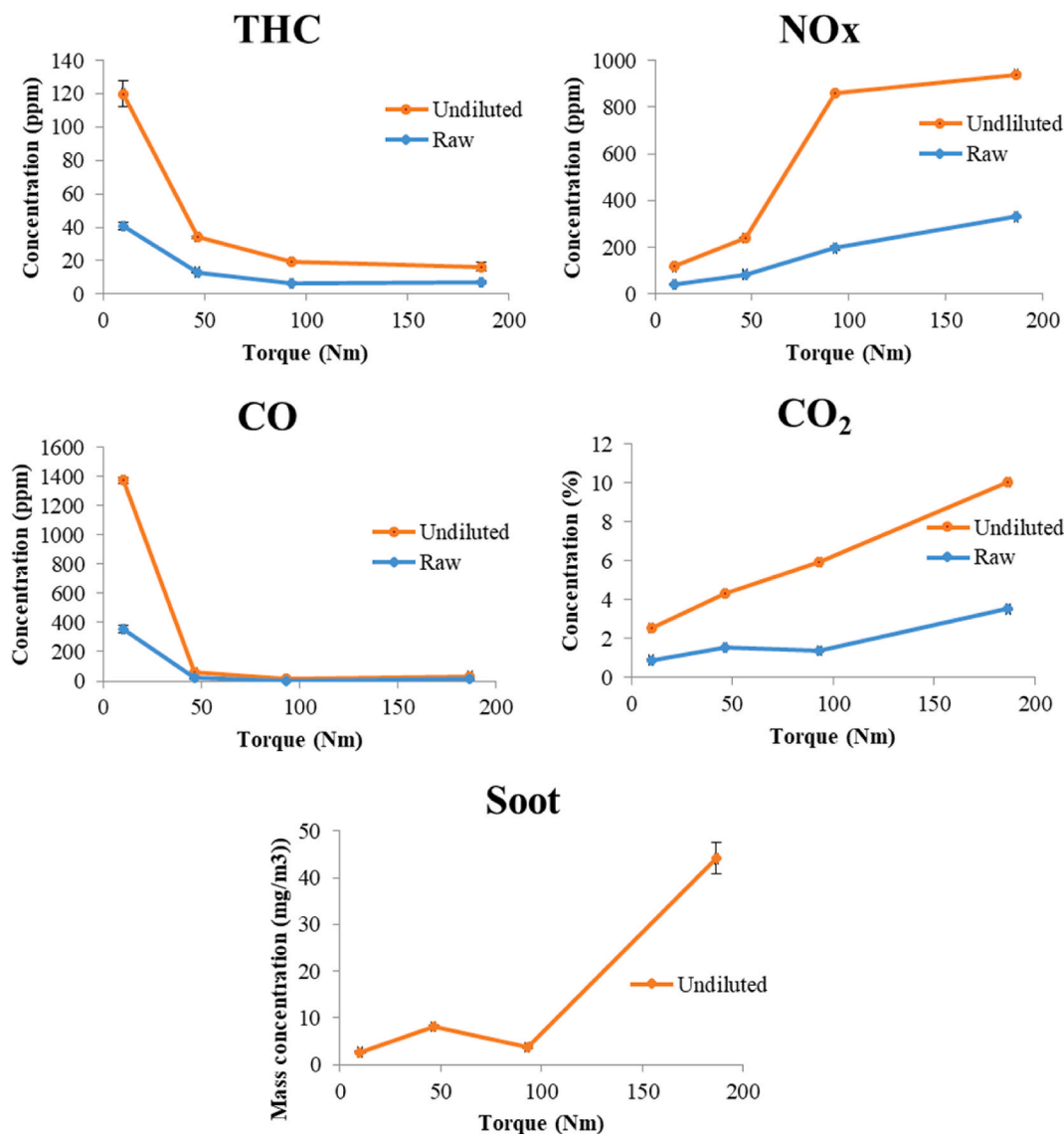
Fig. 5. Concentration of emitted pollutants as a function of engine power.

Table 5
Detected PAH abbreviations and coefficients of variation for trap and filter calibration curves.

PAH	Abbr.	m/z	Trap R^2	Filter R^2
Naphthalene-d8	*IS*	136		
Naphthalene	Nap	128	0.9349	0.9321
Acenaphthylene	Acy	152	0.9998	0.9056
Acenaphthene	Ace	154	0.9864	0.9255
Phenanthrene-d10	*IS*	188		
Fluorene	Flu	166	0.9874	0.9677
Phenanthrene	Phe	178	0.9854	0.9224
Anthracene	Ant	178	0.9410	0.9583
Fluoranthene	FluAn	202	0.9252	0.9883
Pyrene	Pyr	202	0.9607	0.9777
Benz(a)anthracene	BaA	228	0.8284	0.9430
Benzo(a)pyrene	BaP	252	0.9419	0.9734

at high PM loading and possibly also due to the high temperature of 210 °C at the sampling point, this was however corrected for as exact sampling volumes were used to calculate the concentration per m^3.

The dilution effects were more evident in M_A, with a significant difference between the raw and dilute samples. The dilution factors for M_A and M_B, based on total PAH concentrations, were found to be 22.4 and 0.8 respectively. The formation of PAH derivatives in post emission reactions as well as equilibration and particle losses due to impaction along the exhaust extraction ducting can be contributing factors to the noted dilution effects when comparing raw and dilute samples. The post emission reactions would include the formation of alkylated and oxygenated PAHs as well as nitrated PAHs due to the presence of NO_x emissions from the diesel engine. These profiles are reported to be dominated by nitro-naphthalene, 1-nitropyrene and 9-nitroanthracene (Correa et al., 2021; Huang et al., 2015; Kostenidou et al., 2021). The PAH derivative compounds were not quantified in this study although formation of these compounds during dilution and aging would result in lower concentrations of parent PAHs. The particulate PAHs in M_B were 6.36 and 6.19 $\mu g/m^3$ for the raw and dilute sample respectively which shows that there was only a small amount of particulate loss which is likely due to impaction in the exhaust ducting. The secondary trap PAH concentration for the raw M_B (15.7 $\mu g/m^3$) sample is comparable to the primary trap PAH concentration in the M_B dilute sample (14.8 $\mu g/m^3$) which is consistent with the theory that PAHs are transiently associated with particles in the raw exhaust stream and consequently pass through the primary trap. Once these emissions are aged, or have had sufficient

Table 6
LOD and LOQ values for PAHs in gas phase (top) and particulate phase (bottom).

PAH (trap)	pg (trap)		Calculated air sample (ng/m³)	
	LOD	LOQ	LOD	LOQ
Nap	1.4	4.8	0.3	1.0
Acy	3.3	11.1	0.7	2.2
Ace	2.8	9.3	0.6	1.9
Flu	5.1	16.9	1.0	3.4
Phe	8.8	29.3	1.8	5.9
Ant	5.5	18.4	1.1	3.7
Pyr	11.1	36.8	2.2	7.4
FluAn	11.1	36.9	2.2	7.4
BaA	53.8	179.3	10.8	35.9
Chy	51.8	172.6	10.4	34.5
BbF	76.3	254.3	15.3	50.9
BaP	160.2	534.1	32.0	106.8
IcdP	255.2	850.6	51.0	170.1
BghiP	396.6	1322.1	79.3	264.4
DahA	243.2	810.6	48.6	162.1

PAH (filter)	pg (QFF)		Calculated air sample (ng/m3)	
	LOD	LOQ	LOD	LOQ
Nap	1.7	5.7	0.3	1.1
Acy	2.3	7.5	0.5	1.5
Ace	5.7	18.9	1.1	3.8
Flu	2.5	8.2	0.5	1.6
Phe	3.0	9.9	0.6	2.0
Ant	2.2	7.2	0.4	1.4
Pyr	1.5	5.1	0.3	1.0
FluAn	1.3	4.3	0.3	0.9
BaA	7.4	24.8	1.5	5.0
Chy	5.8	19.2	1.2	3.8
BbF	13.1	43.6	2.6	8.7
BaP	38.8	129.4	7.8	25.9
IcdP	71.9	239.8	14.4	48.0
BghiP	69.6	232.0	13.9	46.4
DahA	92.6	308.7	18.5	61.7

Table 7
Concentration of PAHs in raw and dilute exhaust streams in µg/m³.

	PAH	M_A Raw	M_B Raw	M_A Dil	M_B Dil
Primary trap	Nap	2.77	6.99	0.03	13.27
	Acy	0.22	2.46	ND	ND
	Ace	0.25	ND	0.22	ND
	Flu	0.24	2.35	ND	0.21
	Phe	0.30	ND	ND	0.26
	Ant	0.17	ND	ND	0.60
	FluAn	0.21	ND	ND	ND
	Pyr	0.77	ND	ND	0.46
	BaA	0.67	ND	ND	ND
	BaP	ND	ND	ND	ND
	Sum	5.59	11.80	0.25	14.81
Filter	Nap	<DL	6.36	<DL	4.99
	Acy	ND	ND	ND	ND
	Ace	ND	ND	ND	ND
	Flu	ND	ND	ND	ND
	Phe	ND	ND	ND	0.25
	Ant	ND	ND	ND	0.25
	FluAn	ND	ND	ND	ND
	Pyr	ND	ND	ND	0.70
	BaA	ND	ND	ND	ND
	BaP	ND	ND	ND	ND
	Sum	0.00	6.36	0.00	6.19
Secondary trap	Nap	<DL	8.93	<DL	0.15
	Acy	0.22	2.28	ND	ND
	Ace	0.20	2.24	ND	ND
	Flu	0.27	2.28	ND	ND
	Phe	ND	ND	ND	0.23
	Ant	ND	ND	ND	0.12
	FluAn	ND	ND	ND	0.03
	Pyr	ND	ND	ND	0.17
	BaA	ND	ND	ND	ND
	BaP	ND	ND	ND	ND
	Sum	0.69	15.72	0.00	0.70
	Total sum	6.28	33.88	0.25	21.7

time to equilibrate, the PAHs partition from the particulate phase into the more favorable gas phase especially for low molecular weight PAHs, which is then collected on the secondary trap of the raw stream sample and then downwind on the primary trap in the exhaust extraction ducting, respectively.

3.3. PAH profiles

The PAH profiles for M_A and M_B differed significantly in terms of the number, type and concentration of PAHs for both gas and particulate phases. Naphthalene was found to be the most abundant PAH in the raw exhaust stream for both M_A and M_B with a total of 9 PAHs detected in M_A and only 4 in M_B.

Fig. 7 shows that PAHs emitted during idle mode, M_A, ranged from the lighter 2-ringed acenaphthylene to the heavier 4-ringed benzo(a) anthracene and pyrene which were present in the highest concentrations (excluding Nap), none of which were associated with particles.

For M_B (Fig. 8) only lighter 2–3 ringed PAHs up to fluorene were found in the raw exhaust stream but phenanthrene, anthracene, fluoranthene and pyrene were found in the dilute sample stream which were partitioned between gas and particulate phases after mixing with air and having had time to condense and equilibrate. The presence of the lighter PAHs at higher concentrations in the M_B raw stream likely arose from unburnt diesel fuel as during this mode when the throttle is increased there is more fuel introduced into the engine than in idle mode and combustion occurs under more oxygen deficient conditions.

The PAHs emitted during maximum power were found to be predominantly on the filter and secondary trap indicating that they are associated with particles whereas the idle mode produced predominantly gas phase PAH emissions, which was consistent with the soot measurements as seen in Fig. 5 that showed the highest soot concentrations of approximately 44 mg/m³ during maximum power operation,

implying an increased number of adsorption sites for PAHs and thus an increase in transient particle association. The opposite is seen during idle mode where the soot concentrations were negligible thus all PAHs were solely found in the gas phase and were collected on the primary trap.

The PAH profiles in this study were found to be consistent with that of other diesel engine emission studies reported in the literature. In a chassis dynamometer study where vehicle exhaust emissions were sampled under different driving cycles, it was reported that the sum of two-ring, three-ring and four-ring PAHs accounted for ~87% of the total gaseous PAH concentrations (Wei et al., 2015). Dandajeh et al. also reported that the most abundant exhaust PAHs, in a study investigating fuel ignition and injection, were found in the gas phase and consisted of predominantly 2 and 3-ring PAHs (Dandajeh et al., 2019). These findings were consistent with what was reported by other authors, as Hu et al. confirmed that PAHs in the gas phase dominated the total PAH (gas + particle phases) emissions for all the test vehicles in their investigation carried out using a chassis dynamometer under different driving cycles. The authors found that 99% of the 2-ring, 98% of the 3-ring, 97% of the 4-ring and 95% of the carcinogenic PAHs were all found in the gas phase after a diesel particle filter (DPF) which demonstrates the need for gas phase PAH characterisation and quantification (Hu et al., 2013).

3.4. PAH emission factors

Emission factors for M_A and M_B were calculated for each detected PAH in both gas and particulate phases as it was demonstrated in this study that over 80% of PAHs were found in the gas phase, even for the larger 4-ring PAHs.

Light duty vehicle EFs were determined directly from the engine dynamometer measurements using the equation below where the
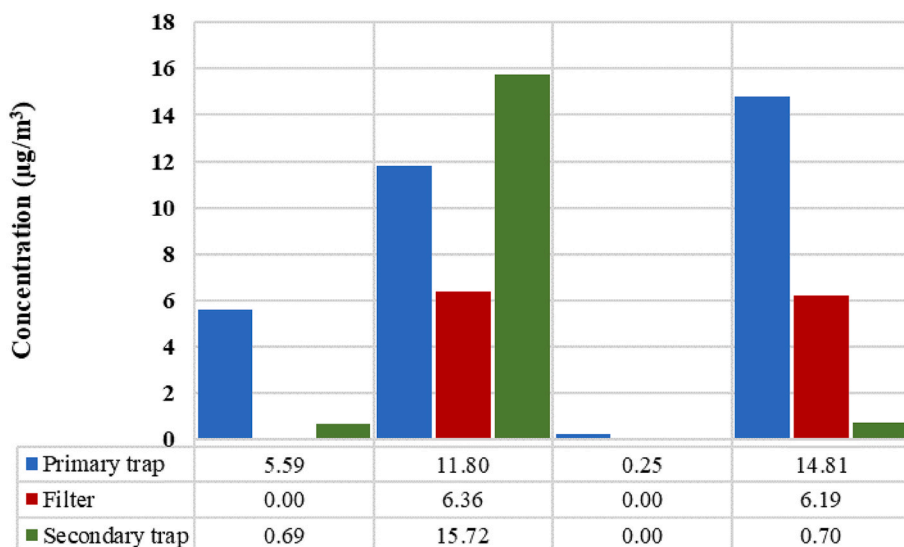
Fig. 6. Total gas and particulate PAH concentrations for raw and dilute samples.
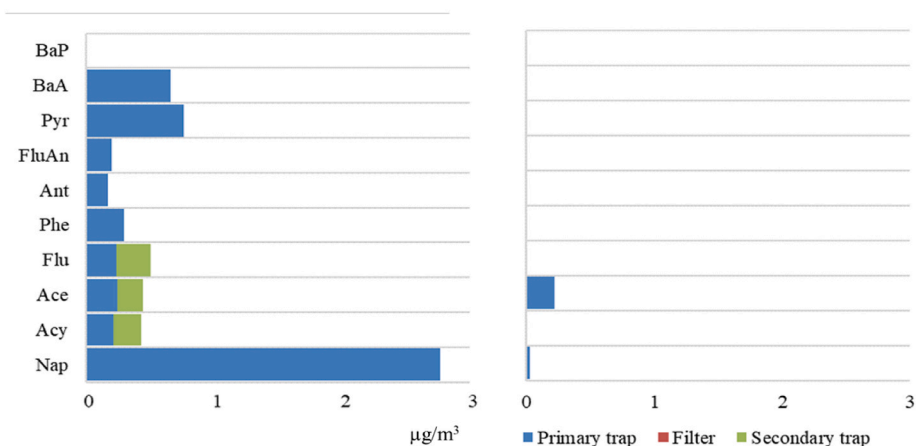

Fig. 7. Idle mode (M_A) PAH profiles for raw (left) and dilute (right) samples.
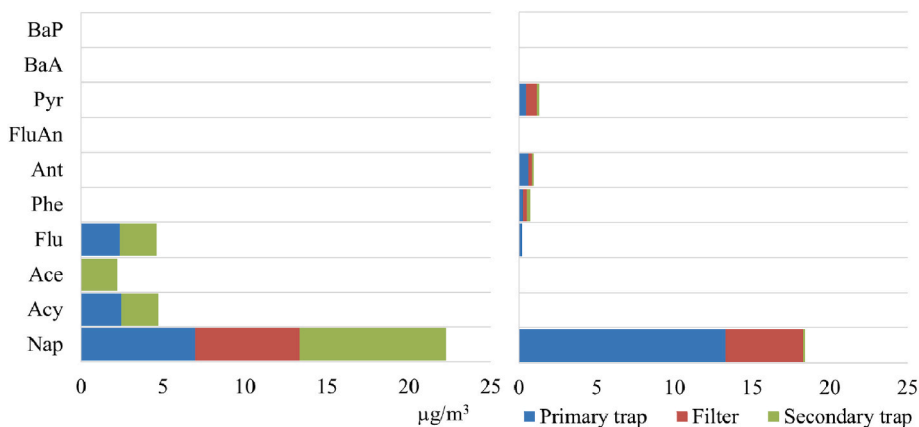

Fig. 8. Max power mode (M_B) PAH profiles for raw (left) and dilute (right) samples.

difference in $[CO_2]$ in the undiluted exhaust stream and the sampling point was used to determine the dilution ratio. The sampling points included dilute emissions in the exhaust duct where there was no in-line CO_2 monitor, therefore the conventional dilution ratio determination approach, using CO_2 as a tracer, could not be adopted. The total air flow that was sampled was also accounted for after the sampling flow rate was taken into account. The sampling correction factor was introduced to correct for the total flow at the sampling point (i.e., what portion of the total air flow was sampled). Otherwise, it would imply that all of the PAHs derived from the fuel combusted were sampled.

Our EFs calculated in this way are noted as being indicative in nature due to the lack of a controlled dilution system for sampling.

Calculation of EFs

$$EF = \frac{[PAH].(\text{Dilution ratio})(\text{Sampling time conversion factor})}{(\text{Ratio of total air sampled})(\text{Fuel consumption})}$$

$$EF_{PAH} = \frac{[PAH].[CO_{2 \text{ undiluted}}][\text{Sampling flow rate}][\text{time conversion factor}]}{[CO_{2 \text{ sampling point}}][\text{Total exhaust flow rate}][\text{Fuel flow rate}]}$$
$$= EF\ (\mu g/kg)$$

Where:

[PAH] = total mass of PAH (μg) on the trap or filter determined from the calibration curve
$[CO_{2 \text{ undiluted}}]$ = concentration (%) of CO_2 in undiluted exhaust
$[CO_{2 \text{ diluted}}]$ = concentration (%) of CO_2 at sampling point
Total exhaust flow rate = average total exhaust mass flow rate (kg/hr).
Sampling flow rate = sampling flow rate (0.5 L per min equates to 0.03 m^3/h atmospheric sampling at 101,8 kPa and temperature at each mode was logged as:
Idle: 25.7 °C.
Max power: 207.2 °C).
Time factor = factor of 6 used to convert 10 min sampling time to 1 h.
Fuel flow rate = fuel consumption measured by Sasol automated system:
Idle: 0.300 kg/h.
Max power: 18.400 kg/h.
EF_{PAH} = the PAH emission factor (μg of PAH emitted per kg of fuel burned).

From Table 8 and previous results and discussion, it is evident that the mode of engine operation has a significant influence on the type and number of PAHs emitted. The idle mode resulted in a total PAH EF of 1181.14 μg/kg which is significantly higher than the total PAH EF of 592.10 μg/kg determined during maximum power mode. The vast differences in parameters between the two engine operational modes play a major role on the resultant EF i.e., the maximum power mode required

Table 8
Calculated emission factors for PAHs emitted per kg fuel burned during idle and maximum power mode.

Idle mode	PAH	[μg/m³]	EF (μg/kg)
1° trap	Nap	2.77	520.15
	Acy	0.22	41.31
	Ace	0.25	46.95
	Flu	0.24	45.07
	Phe	0.3	56.33
	Ant	0.17	31.92
	FluAn	0.21	39.43
	Pyr	0.77	144.59
	BaA	0.67	125.81
2° trap	Nap	–	–
	Acy	0.22	41.31
	Ace	0.2	37.56
	Flu	0.27	50.70
	Total	6.29	1181.14
Max power mode	PAH	[μg/m³]	EF (μg/kg)
1° trap	Nap	6.99	122.02
	Acy	2.46	42.94
	Flu	2.35	41.02
Filter	Nap	6.39	111.54
2° trap	Nap	8.93	155.88
	Acy	2.28	39.80
	Ace	2.24	39.10
	Flu	2.28	39.80
	Total	33.92	592.10

over 60 times more fuel, which results in a lower EF.

3.5. Comparison to other studies

The EFs in this study were compared to the EFs obtained from other studies whereby on-road methodologies were used and only particulate emissions were measured. It must be noted that this study was a stationary test using one type of fuel whereas the other studies where on-road real time tests where the average of emissions from many vehicles were therefore measured. Whilst it is acknowledged that chassis-based study results would have yielded very useful comparisons, unfortunately other studies in literature, including those for chassis studies, use distance-based EF which are thus not directly comparable to the results generated in this study. Only reported studies reporting volume based EFs (i.e., with μg/kg units) were thus included, as they allow for direct comparison.

A comprehensive comparison of the particle associated PAHs from diesel exhaust showed that EFs reported over the past several decades span up to 8 orders of magnitude (Hays et al., 2017). It is immediately evident from the EFs in Table 9 and from Fig. 9 that there are significant differences in reported emission factors from various studies which is likely due to the way the test was conducted as well as the factors influencing the emissions such as the type of fuel that was used. The sampling volumes used in each study are substantially different and it must be noted that larger sample volumes are needed to obtain concentrations above LOD values for particle phase samples. In this study a sampling volume of 5 L with a low sampling flow rate of 500 mL/min was applied whereas high flow rates of 450 L/min, 30–450 L/min, and 50 L/min were applied for several hours in the tunnel, freeway and on-road study, respectively (Marr et al., 1999; Phuleria et al., 2006; Ning et al., 2008).

Other authors found that 95% of the total measured particulate emission factors were as a result of 3 and 4-ring PAHs (Zheng et al., 2017), which was consistent with what was found in this study where all particulate PAHs were found to be the lower molecular weight moieties. It must be noted that 89% of EFs were accounted for from gas phase PAHs during idle mode and 35% during the max power mode, of which 3 and 4-ring PAHs were also predominant although heavier PAHs such as pyrene and benz(a)anthracene were detected.

Testing an individual vehicle in a controlled setting such as in this study, or even averaging over several vehicles, can lead to very different results than a tunnel study that includes an average over thousands of vehicles equipped with numerous engine types and burning different fuels, which must be taken into consideration. A chassis dynamometer study was conducted by Wei et al. whereby PAHs in vehicular exhaust were characterized and quantified whilst the engine was operated under different driving cycles including idle and acceleration mode, such as in this study. The authors confirmed that emissions are influenced by the mode of engine operation and found that the concentration of PAHs was the highest in acceleration tests, followed by deceleration and idle tests. The sum of 2–4 ring PAHs accounted for 87% of the total gaseous PAH concentration which was consistent with this study (Wei et al., 2015). When considering EFs from vehicles within different European classes, it was found that PAH emissions vary according to the Euro standard of the vehicle, with the oldest Euro standard displaying the highest emissions. In the case of diesel private cars, ΣPAHs EF was found to be 26.78 ± 10.85 mg km^{-1} for Euro 1, 3.09 ± 3.26 mg km^{-1} for EURO 2, and 1.29 ± 0.49 mg km^{-1} for Euro 3 (Perrone et al., 2014). The higher EFs reported in this study can be expected as the engine employed is older in order to represent engines in operation in developing countries, and they are thus complaint to older European engine classes and standards (Liu et al., 2017).

What is evidently conclusive from this comparison is that the gas phase EFs, which are not considered in any other study, are comparable and in some cases higher than the particulate EFs especially for lower molecular weight PAHs. Fig. 9 reveals that the PAH EF profiles are

Table 9

Comparison of PAH EFs (in μg/kg fuel burned) obtained from various studies done on light duty vehicles (LDVs).

PAH	This study (gas + particle)		This study (particle)		This study (gas)		Tunnel study[a] (particle)		Freeway[b] (particle)		On road[c] (particle)	
	M_A	M_B	M_A	M_B	M_A	M_B	Ultrafine	Accum.	CA-110	I-710	1996a	1997a
Nap	520.15	389.44		267.42	520.15	122.02						
Acy	82.62	82.74	41.31	39.80	41.31	42.94						
Ace	84.50	39.10	37.56	39.10	46.95							
Flu	95.77	80.82	50.70	39.80	45.07	41.02	2.39	0.37	2.86	16.29	8.00	10.30
Phe	56.33				56.33							
Ant	31.92				31.92							
FluAn	39.43				39.43							
Pyr	144.59				144.59		3.63	0.55	3.30	23.21	9.00	13.8
BaA	125.81				125.81		4.11	0.43	0.43	12.24	4.80	8.80
BaP							5.08	0.34	0.40	3.52	6.40	8.30

[a] Phuleria et al., (2006): EF attributable to LDVs in Ultrafine (particles with aerodynamic diameters (Dp) < 0.18 μm) and Accumulation Mode (Dp < 2.5 μm).

[b] Ning et al., (2008): Freeway EFs in $PM_{2.5}$ samples collected from California State Highway (CA-110: only light-duty gasoline-powered vehicles) and the Long Beach Freeway (I-710: 80% light-duty gasoline-powered vehicles).

[c] Marr et al., (1999) On-Road Emission Factors for Particle-Phase PAHs for light-duty vehicles (μg/kg) for 1996 (associated with particles <1.3 μm aerodynamic diameter (PM1.3), not background-subtracted) and 1997 (Background-subtracted PAH associated with particles<2.5 μm aerodynamic diameter (PM2.5).
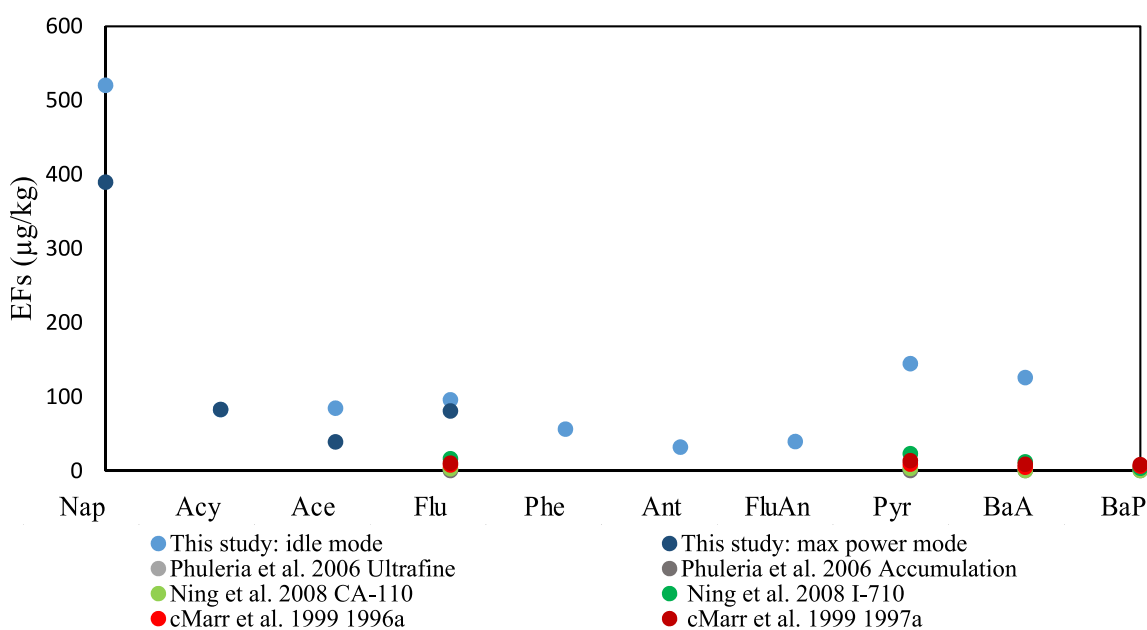

Fig. 9. Comparison of particulate PAH EFs (in μg/kg fuel burned) obtained from various studies done on LDVs where this study represents a sum of gas and particle phase.

significantly different when the gas phase is considered whereas the profiles for all the other studies showed prevalence of heavier PAHs such as pyrene, benz(a)anthracene and benzo(a)pyrene. The fluorene EF was significantly higher in this study when compared to the tunnel study suggesting that fluorene exists in both phases.

A direct comparison is not possible due to the differences in the sampling methods and environments in which measurements were taken, however the EF profiles and the variance in the EF values demonstrate the necessity to include both gas and particulate emissions for an accurate assessment of the potential impact transportation may have on human and environmental health.

4. Conclusion

In view of the adverse environmental and health impacts of airborne PAHs that are sourced from diesel exhaust, it is crucial that accurate assessment of the effects of their concentrations be carried out and emission factors be determined to establish appropriate management and mitigation strategies. PAHs vary in physiochemical properties and they have been found to co-exist in both particulate and gas phases

which makes the sampling, extraction and analysis techniques required for the monitoring thereof somewhat challenging.

In this engine dynamometer study, the simultaneous sampling of gas and particulate PAHs from diesel exhaust emissions was successfully achieved by portable denuder devices consisting of a QFF sandwiched between two multichannel PDMS traps. The traps and filter were individually thermally desorbed and analysed by comprehensive two-dimensional gas chromatography with time-of-flight mass spectrometric detection. The sampling was rapid and effective and low limits of detection for PAHs were found for the experimental method ranging from 0.3 to 18.5 ng/m^3 for filters and 0.3–79.3 ng/m^3 for PDMS traps. Dynamometer studies have the advantage of being able to investigate vehicle emissions under different load settings in a controlled laboratory environment that is free from other sources, however a limitation to this study is that no PAH emissions arising from elsewhere on the vehicle aside from the engine are considered, such as wear of brake linings and tyres, as well as re-suspended road dust, which also have an impact on the PAH emissions from vehicle operation. It should also be noted that there was no size resolution of sampled particulate matter in this study, as total PM was collected.

The PAH profiles for each mode differed significantly in terms of the number, type and concentration of PAHs. Total PAH EFs (gas and particle phase) were determined to be 1181.14 and 592.10 μg/kg for the idle and maximum power mode respectively. Naphthalene was found to be the most abundant PAH in the raw exhaust stream for both modes and a total of 9 PAHs were detected in the idle mode and only 4 in maximum power mode. The maximum power mode revealed the highest concentration of particulate PAHs which correlated with elevated soot measurements. The presence of smaller 2–3 ringed PAHs in the exhaust may originate from unburned diesel fuel but the presence of the larger 4–6 ringed PAHs, that are not typically present in the fuel, suggest that they originate from other sources such as pyrosynthesis or the lubricating oil.

Over 80% of PAHs were found in the gas phase which emphasized the need for this study seeing that numerous other studies tend to focus only on particulate matter in the determination of PAH emission factors. Gas phase PAHs can undergo oxidation reactions producing secondary organic aerosol compounds which in some cases have been found to be more toxic than the precursor compounds (Lin et al., 2019). Therefore, characterizing the EFs of PAHs, the phase partitioning of these compounds, as well as transformations thereof, are important to air quality control as well as the health of the general public.

For future work it is recommended that a study be conducted with a controlled dilution ratio and additional tests should be carried out to more accurately determine the extent of blow off and transient phase associations at different operating modes and engine temperatures. An in-depth look into the formation of PAH derivatives and their quantification would be very valuable as low molecular weight PAHs, which were found to be more abundant, can react with NO_x in the exhaust to form highly toxic nitrated and oxygenated PAH compounds that have adverse human health and environmental effects (Keyte et al., 2016).

CRediT authorship contribution statement

G. Geldenhuys: Methodology, Investigation, Formal analysis, Writing – original draft. **M. Wattrus:** Methodology, Resources, Investigation, Formal analysis, Writing – review & editing. **P.B.C. Forbes:** Conceptualization, Methodology, Investigation, Formal analysis, Writing – review & editing, Supervision, Project administration, Resources, Funding acquisition.

Declaration of competing interest

The authors declare that they have no known competing financial interests or personal relationships that could have appeared to influence the work reported in this paper.

Acknowledgements

References

Abu-Allaban, M., Coulomb, W., Gertler, A., Gillies, J., Pierson, W., Rogers, C., Sagebiel, J., Tarnay, L., 2002. Exhaust particle size distribution measurements at the Tuscarora Mountain tunnel. Aerosol. Sci. Technol. 36, 771e789.

Abu-Allaban, M., Gillies, J.A., Gertler, A.W., Clayton, R., Proffitt, D., 2003. Tailpipe resuspended road dust, and brake-wear emission factors from on-road vehicles. Atmos. Environ. 37, 5283e5293.

Allen, J.O., Mayo, P.R., Hughes, L.S., Salmon, L.G., Cass, G.R., 2001. Emissions of size-segregated aerosols from on-road vehicles in the Caldecott Tunnel. Environ. Sci. Technol. 35, 4189–4197.

Ayetor, G.K., Mbonigaba, Innocent, Ampofo, Joshua, Albert, Sunnu, 2021. Investigating the state of road vehicle emissions in Africa: a case study of Ghana and Rwanda. Transportation Research Interdisciplinary Perspectives 11, 100409.

Burgard, D.A., Bishop, G.A., Williams, M.J., Stedman, D.H., 2003. On-road Remote Sensing of Automobile Emissions in the Denver Area: Year 4, January 2003. University of Denver.

Cocker, D.R., Shah, S.D., Johnson, K., Miller, J.W., Norbeck, J.M., 2004. Development and application of a mobile laboratory for measuring emissions from diesel engines. 1. Regulated gaseous emissions. Environ. Sci. Technol. 38 (7), 2182–2189.

Correa, S.M., Arbilla, G., da Silva, C.M., Martins, E.M., de Souza, S.L.Q., 2021. Determination of size-segregated polycyclic aromatic hydrocarbon and its nitro and alkyl analogs in emissions from diesel-biodiesel blends. Fuel 283, 118912.

Dandajeh, Adamu, Hamisu, Talibi, Midhat, Ladommatos, Nicos, Paul, Hellier, 2019. 'Influence of combustion characteristics and fuel composition on exhaust PAHs in a compression ignition engine. Energies 12, 2575.

Eiguren-Fernandez, A., Miguel, A.H., 2012. Size-resolved polycyclic aromatic hydrocarbon emission factors from on-road gasoline and diesel vehicles: temperature effect on the nuclei-mode. Environ. Sci. Technol. 46, 2607–2615.

Forbes, P.B.C., Rohwer, E.R., 2009. Investigations into a novel method for atmospheric polycyclic aromatic hydrocarbon monitoring. Environ. Pollut. 157 (8–9), 2529–2535.

Forbes, P.B.C., Rohwer, E.R., 2015. In: Forbes, Patricia (Ed.), Chapter 5: Denuders, in Comprehensive Analytical Chemistry Vol. 70: Monitoring of Air Pollutants: Sampling, Sample Preparation and Analytical Techniques, vol. 70. Netherlands: Elsevier, Netherlands, ISBN 978-0-444-63553-2, pp. 153–181.

Forbes, P.B.C., Karg, E.W., Zimmermann, R., Rohwer, E.R., 2012. The use of multi-channel silicone rubber traps as denuders for polycyclic aromatic hydrocarbons. Anal. Chim. Acta 730, 71–79.

Forbes, P.B.C., Karg, E.W., Geldenhuys, G., Nsibande, S.A., Zimmermann, R., Rohwer, E. R., 2013. Characterisation of atmospheric semi-volatile organic compounds. Clean Air J. 23 (1), 3–6. ISSN 1017-1703.

Geldenhuys, G., 2014. Characterization of Diesel Emissions with Respect to Semi-volatile Organic Compounds in South African Platinum Mines and Other Confined Environments. MSc Thesis, The University of Pretoria viewed 5 March 2017. http://hdl.handle.net/2263/46248.

Geldenhuys, G., Rohwer, E.R., Naudé, Y., Forbes, P.B.C., 2015. Monitoring of atmospheric gaseous and particulate polycyclic aromatic hydrocarbons in South African platinum mines utilizing portable denuder sampling with analysis by thermal desorption–comprehensive gas chromatography mass spectrometry. J. Chromatogr. A 1380, 17–28.

Gietl, J.K., Lawrence, R., Thorpe, A.J., Harrison, R.M., 2010. Identification of brake wear particles and derivation of a quantitative tracer for brake dust at a major road. Atmos. Environ. 44, 141–146.

Guo, H., Zhang, Q., Shi, Y., Wang, D., 2007. On-road Remote Sensing Measurements and Fuel Based Motor Vehicle Emission Inventory in Hangzhou, China, vol. 41. Atmospheric Environment, pp. 3095–3107.

Handler, M., Puls, C., Zbiral, J., Marr, I., Puxbaum, H., Limbeck, A., 2008. Size and composition of particulate emissions from motor vehicles in the Kaisermühlen-Tunnel. Atmos. Environ. 42, 2173–2186.

Hays, Michael D., Preston, William, J George, Barbara, J George, Ingrid, Snow, Richard, Faircloth, James, Long, Thomas, Baldauf, Richard W., McDonald, Joseph, 2017. 'Temperature and driving cycle significantly affect carbonaceous gas and particle matter emissions from diesel trucks. Energy Fuels 31, 11034–11042.

Huang, L., Bohac, S.V., Chernyak, S.M., Batterman, S.A., 2015. Effects of fuels, engine load and exhaust after-treatment on diesel engine SVOC emissions and development of SVOC profiles for receptor modeling. Atmos. Environ. 102, 228–238.

Hu, Shaohua, Jorn, D., Herner, Robertson, William, Kobayashi, Reiko, Chang, M-C Oliver, Huang, Shiou-mei, Zielinska, Barbara, Norman, Kado, Collins, John F., Paul, Rieger, 2013. 'Emissions of polycyclic aromatic hydrocarbons (PAHs) and nitro-PAHs from heavy-duty diesel vehicles with DPF and SCR. J. Air Waste Manag. Assoc. 63, 984–996.

International Agency for Research on Cancer (IARC), 2012. Diesel Engine Exhaust Carcinogenic 2012a. Press Release, p. 213.

International Agency for Research on Cancer (IARC), World Health Organization (WHO), 2014. Diesel and gasoline engine exhausts and some nitroarenes (volume 105). Available at. http://monographs.iarc.fr/ENG/Monographs/vol105/mono105.pdf.

International Agency for Research on Cancer (IARC), World Health Organization (WHO), 2012. IRAC: Diesel Engine Exhaust Carcinogenic (press release). Available at. https://www.iarc.fr/en/media-centre/pr/2012/pdfs/pr213_E.pdf.

Kim, K.H., Jahan, S.A., Kabir, E., Brown, R.J.C., 2013. A review of airborne polycyclic aromatic hydrocarbons (PAHs) and their human health effects. Environ. Int. 60, 71–80.

Keyte, Ian J., Albinet, Alexandre, Harrison, Roy M., 2016. 'On-road traffic emissions of polycyclic aromatic hydrocarbons and their oxy-and nitro-derivative compounds measured in road tunnel environments. Sci. Total Environ. 566, 1131–1142.

Kostenidou, E., Martinez-Valiente, A., R'mili, B., Marques, B., Temime-Roussel, B., Durand, A., André, M., Liu, Y., Louis, C., Vansevenant, B., Ferry, D., 2021. Emission factors, chemical composition, and morphology of particles emitted from Euro 5 diesel and gasoline light-duty vehicles during transient cycles. Atmos. Chem. Phys. 21 (6), 4779–4796.

Kristensson, A., Johansson, C., Westerholm, R., Swietlicki, E., Gidhagen, L., Wideqvist, U., Vesely, V., 2004. Real-world traffic emission factors of gases and particles measured in a road tunnel in Stockholm, Sweden. Atmos. Environ. 38, 657–6773.

Kumari, K Maharaj, Lakhani, Anita, 2018. PAHs in Gas and Particulate Phases: Measurement and Control', Environmental Contaminants. Springer.

Lin, Yuan-Chung, Ching Li, Ya, Amesho, Kassian TT., Chou, Feng-Chih, Cheng, Pei-Cheng, 2019. 'Characterization and quantification of PM2. 5 emissions and PAHs

concentration in PM2. 5 from the exhausts of diesel vehicles with various accumulated mileages. Sci. Total Environ. 660, 188–198.

Liu, Y., Martinet, S., Louis, C., Pasquier, A., Tassel, P., Perret, P., 2017. Emission characterization of in-use diesel and gasoline Euro 4 to Euro 6 passenger cars tested on chassis dynamometer bench and emission model assessment. Aerosol Air Qual. Res. 17, 2289–2299.

Mancilla, Y., Mendoza, A., 2012. A tunnel study to characterize PM2. 5 emissions from gasoline-powered vehicles in Monterrey, Mexico. Atmos. Environ. 59, 449–460.

Marr, L.C., Kirchstetter, T.W., Harley, R.A., Miguel, A.H., Hering, S.V., Hammond, S.K., 1999. Characterization of polycyclic aromatic hydrocarbons in motor vehicle fuels and exhaust emissions. Environ. Sci. Technol. 33 (18), 3091–3099.

Morawska, L., Zhang, J.J., 2002. Combustion sources of particles. 1. Health relevance and source signatures. Chemosphere 49, 1045–1058.

Munyeza, Chiedza F., Kohlmeier, Vesta, Dragan, George C., Karg, Erwin W., Rohwer, Egmont R., Zimmermann, Ralf, Forbes, Patricia BC., 2019. 'Characterisation of particle collection and transmission in a polydimethylsiloxane based denuder sampler. J. Aerosol Sci. 130, 22–31.

National Center for Biotechnology Information. PubChem database. Available at. https://pubchem.ncbi.nlm.nih.gov/compound.

Ning, Z., Polidori, A., Schauer, J.J., Sioutas, C., 2008. Emission factors of PM species based on freeway measurements and comparison with tunnel and dynamometer studies. Atmos. Environ. 42, 3099–3114.

Oliveira, C., Pio, C., Caseiro, A., Santos, P., Nunes, T., Mao, H., Luahana, L., Sokhi, R., 2010. Road traffic impact on urban atmospheric aerosol loading at Oporto, Portugal. Atmos. Environ. 44, 3147–3158.

Ono-Ogasawara, M., Smith, T.J., 2004. Diesel exhaust particles in the work environment and their analysis. Ind. Health 42 (4), 389–399.

Pandey, S.K., Kim, K., Brown, R.J.C., 2011. A review of techniques for the determination of polycyclic aromatic hydrocarbons in air. Trends Anal. Chem. 30 (11), 1716–1739.

Perrone, Maria Grazia, Carbone, Claudio, Faedo, Davide, Ferrero, Luca, Maggioni, Angela, Sangiorgi, Giorgia, Bolzacchini, Ezio, 2014. 'Exhaust emissions of polycyclic aromatic hydrocarbons, n-alkanes and phenols from vehicles coming within different European classes. Atmos. Environ. 82, 391–400.

Pey, J., Querol, X., Alastuey, A., 2010. Discriminating the regional and urban contributions in the North-Western Mediterranean: PM levels and composition. Atmos. Environ. 44, 1587–1596.

Phuleria, H.C., Geller, M.D., Fine, P.M., Sioutas, C., 2006. Size resolved emissions of organic tracers from light- and heavy duty vehicles measured in a California roadway tunnel. Environ. Sci. Technol. 40 (13), 4109–4118.

Poster, D.L., Schantz, M.M., Sander, L.C., Wise, S.A., 2006. Analysis of polycyclic aromatic hydrocarbons (PAHs) in environmental samples: a critical review of gas chromatographic (GC) methods. Anal. Bioanal. Chem. 386, 859–881.

Rengarajan, T., Rajendran, P., Nandakumar, N., Lokeshkumar, B., Rajendran, P., Nishigaki, I., 2015. Exposure to polycyclic aromatic hydrocarbons with special focus on cancer. Asian Pacific J. Tropic. Biomed. 5 (3), 182–189. https://doi.org/10.1016/S2221-1691(15)30003-4. ISSN 2221-1691.

Rhead, M.M., Pemberton, R.D., 1996. Sources of naphthalene in diesel exhaust emissions. Energy Fuel. 10 (3), 837–843.

Reşitoğlu, Aslan, İbrahim, Altinişik, Kemal, Ali, Keskin, 2015. The pollutant emissions from diesel-engine vehicles and exhaust aftertreatment systems. Clean Technol. Environ. Policy 17, 15–27.

Riccio, A., Chianese, E., Monaco, D., Costagliola, M.A., Perretta, G., Prati, M.V., Agrillo, G., Esposito, A., Gasbarra, D., Shindler, L., Brusasca, G., Nanni, A., Pozzi, C.,

Magliulo, V., 2016. Real-world automotive particulate matter and PAH emission factors and profile concentrations: results from an urban tunnel experiment in Naples. Italy. Atmos. Environ. 141, 379–387.

Rohr, A.C., Wyzga, R.E., 2012. Attributing health effects to individual particulate matter constituents. Atmos. Environ. 62, 130–152.

Samet, J.M., Dominici, F., Curriero, F.C., Coursac, I., Zeger, S.L., 2000. Fine particulate air pollution and mortality in 20 US Cities, 1987–1994. N. Engl. J. Med. 343 (24), 1742–1749.

Schifter, I., Díaz, L., Durán, J., Guzmán, E., Chávez, O., López-Salina, E., 2003. Remote sensing study of emissions from motor vehicles in the metropolitan area of Mexico City. Environ. Sci. Technol. 37, 395–401.

Shen, H., Tao, S., Liu, J., Huang, Y., Chen, H., Li, W., Zhang, Y., Chen, Y., Su, S., Lin, N., Xu, Y., 2014. Global lung cancer risk from PAH exposure highly depends on emission sources and individual susceptibility. Sci. Rep. 4, 6561.

U.S. Environmental Protection Agency (EPA, 2004. Air Quality Criteria for Particulate Matter. US Environmental Protection Agency, Research Triangle Park.

U.S. National Toxicology Program (NTP), 2014. Report on Carcinogens, thirteenth ed. Available at. http://ntp.niehs.nih.gov/pubhealth/roc/roc13.

Vicente Franco, V., Kousoulidou, M., Muntean, M., Ntziachristos, L., Hausberger, S., Dilara, P., 2013. Road Vehicle Emission Factors Development: A Review, vol. 70. Atmospheric Environment, pp. 84–97.

Vione, D., Barra, S., de Gennaro, G., de Rienzo, M., Gilardoni, S., Perrone, M.G., Pozzoli, L., 2004. Polycyclic aromatic hydrocarbons in the atmosphere: monitoring, sources, sinks and fate. Ann. Chim. 94, 17–32.

Wang, Bei, Lau, Yik-Sze, Huang, Yuhan, Organ, Bruce, Chuang, Hsiao-Chi, Ho, Steven Sai Hang, Qu, Linli, Lee, Shun-Cheng, Ho, Kin-Fai, 2021. 'Chemical and toxicological characterization of particulate emissions from diesel vehicles. J. Hazard Mater. 405, 124613.

Wang, X., Westerdahl, D., Wu, Y., Pan, X., Zhang, K.M., 2011. On-road emission factor distributions of individual diesel vehicles in and around Beijing, China. Atmos. Environ. 45, 503–513.

Wei, Hu, Liu, Guangbin, Tu, Yong, Zhong, Qin, 2015. 'Emission of polycyclic aromatic hydrocarbons from different types of motor vehicles' exhaust. Environ. Earth Sci. 74, 5557–5564.

Weitekamp, Chelsea A., Kerr, Lukas B., Dishaw, Laura, Nichols, Jennifer, Lein, McKayla, Stewart, Michael J., 2020. 'A systematic review of the health effects associated with the inhalation of particle-filtered and whole diesel exhaust. Inhal. Toxicol. 32, 1–13.

Weingartner, E., Keller, C., Stahel, W., Burtscher, H., Baltensperger, U., 1997. Aerosol emission in a road tunnel. Atmos. Environ. 31 (3), 451–462.

Yanowitz, J., Graboski, M.S., Ryan, L.B., Alleman, T.L., McCormick, R.L., 1999. Chassis dynamometer study of emissions from 21 in-use heavy-duty diesel vehicles. Environ. Sci. Technol. 33 (2), 209–216.

Zhang, Y., Stedman, D.H., Bishop, G.A., Guenther, P.L., Beaton, S.P., 1995. Worldwide on-road vehicle exhaust emissions study by remote sensing. Environ. Sci. Technol. 29, 2286–2294.

Zheng, X., Wu, Y., Zhang, S., Baldauf, R.W., Zhang, K.M., Hu, J., Li, Z., Fu, L., Hao, J., 2016. Joint measurements of black carbon and particle mass for heavy-duty diesel vehicles using a portable emission measurement system. Atmos. Environ. 141, 435–442.

Zheng, X., Wu, Y., Zhang, S., Hu, J., Max Zhang, K., Li, Z., He, L., Hao, J., 2017. Characterizing particulate polycyclic aromatic hydrocarbon emissions from diesel vehicles using a portable emissions measurement system. Sci. Rep. 7 (10058), 1–12. https://doi.org/10.1038/s41598-017-09822.